Acta Cryst. (1998). B**54**, 320–329

Carbonyl–Carbonyl Interactions can be Competitive with Hydrogen Bonds

FRANK H. ALLEN,[a]* CHRISTINE A. BAALHAM,[a] JOS P. M. LOMMERSE[a] AND PAUL R. RAITHBY[b]

[a]*Cambridge Crystallographic Data Centre, 12 Union Road, Cambridge CB2 1EZ, England, and* [b]*Department of Chemistry, University of Cambridge, Lensfield Road, Cambridge CB2 1EW, England. E-mail: allen@ccdc.cam.ac.uk*

(*Received 25 September 1997; accepted 22 January 1998*)

Abstract

The geometries and attractive energies of carbonyl–carbonyl interactions have been investigated using crystallographic data and *ab initio* molecular-orbital calculations. Analysis of crystallographic data for 9049 carbon-substituted >C=O groups shows that 1328 (15%) form contacts with other >C=O groups, in which $d(C\cdots O) < 3.6$ Å. Three common interaction motifs are observed in crystal structures: (*a*) a slightly sheared antiparallel motif (650 instances) involving a pair of short C···O interactions, together with (*b*) a perpendicular motif (116 instances) and (*c*) a highly sheared parallel motif (130 instances), which both involve a single short C···O interaction. Together, these motifs account for 945 (71%) of the observed interactions. *Ab-initio*-based molecular-orbital calculations (6-31G** basis sets), using intermolecular perturbation theory (IMPT) applied to a bis-propanone dimer model, yield an attractive interaction energy of -22.3 kJ mol^{-1} for a perfect rectangular antiparallel dimer having both $d(C\cdots O) = 3.02$ Å and attractive energies < -20 kJ mol^{-1} over the $d(C\cdots O)$ range 2.92–3.32 Å. These energies are comparable to those of medium-strength hydrogen bonds. The IMPT calculations indicate a slight shearing of the antiparallel motif with increasing $d(C\cdots O)$. For the perpendicular motif, IMPT yields an attractive interaction energy of -7.6 kJ mol^{-1}, comparable in strength to a C—H···O hydrogen bond and with the single $d(C\cdots O)$ again at 3.02 Å.

1. Introduction

Carbonyl groups are ubiquitous in organic and biological systems and their molecular recognition properties have been studied extensively. Much of this work has concerned the relative hydrogen-bond acceptor abilities of >C=O in various chemical environments, *e.g.* ketones, carboxylic acids, amides *etc.*, and on the directional preferences and strengths (*ca.* -20 to -30 kJ mol^{-1}) of these interactions (see Jeffrey & Saenger, 1991, for leading references). However, there is a growing body of literature that is concerned with non-covalent interactions of the >C(δ+)—O(δ−) dipole that are not mediated by hydrogen. Bolton (1963, 1964, 1965) showed that intermolecular N—H···O hydrogen bonds did not occur in the crystal structure of alloxan, the extended structure being determined instead by intermolecular carbonyl···carbonyl interactions. Later, Bernstein *et al.* (1974) identified a tendency for quinonoidal carbonyl groups to interact either through C—H···O hydrogen bonding or through the O(δ−)···C(δ+)=O perpendicular interaction motif (I). This interaction, of course, models the approach of an oxygen nucleophile to a carbonyl centre, a system that was analysed by Bürgi *et al.* (1974) in their studies of chemical reactions pathways using crystallographic data. They found typical O···C=O approach angles of 100–110°.

Taylor *et al.* (1990) highlighted the value of crystallographic data for suggesting isosteric replacements in modelling protein–ligand interactions and constructed composite crystal-field environments for carbonyl and nitro groups. Their work showed that many of the short intermolecular contacts made by carbonyl groups are to other carbonyl groups in the extended crystal structure; they identified the perpendicular motif (I) noted above and also the antiparallel arrangements (II). At the same time, Gavezzotti (1990) published a study of the packing arrangements of 80 crystal structures containing C, H and one carbonyl group only. He showed that the antiparallel motif (II) was common and permitted the close approach of >C=O groups. Pure lattice translations or, predominantly, the presence of a centre of symmetry, generated perfect antiparallelism in the crystal structures. He found no examples of motif (I) in his sample, but noted the sheared parallel motif (III) at longer C···O separations.

More recently, Maccallum *et al.* (1995*a*,*b*) have demonstrated the importance of Coulombic interactions between the C and O atoms of proximal CONH groups in proteins as an important factor in stablizing α-helices, β-sheets and the right-hand twist often observed in β-strands. Their calculations indicate an attractive carbonyl···carbonyl interaction energy of *ca.* -8 kJ mol^{-1} in specific cases and remark that these interactions are *ca.* 80% as strong as the CO···HN hydrogen bonds within their computational model.

In this paper we examine the geometrical evidence for non-covalent interactions between carbonyl groups that can be derived from the small molecule crystal structures available in the Cambridge Structural Database (CSD: Allen *et al.*, 1991). Further, we also calculate interaction energies between carbonyl groups using *ab-initio*-based molecular-orbital methods at the 6-31G** basis set level and the intermolecular perturbation theory of Hayes & Stone (1984). Interaction motifs, and their geometries, determined from the database analysis are used to guide the computational studies. The combination of database analysis and high-level molecular-orbital calculations is a powerful one and has recently provided significant insights into the nature of a variety of non-covalent interactions, *e.g.* halogen···O=C *etc.* (Lommerse *et al.*, 1996), halogen···O(nitro) (Allen, Lommerse *et al.*, 1997) and N,O—H···O(nitro) hydrogen bonds (Allen, Baalham *et al.*, 1997).

2. Methodology

2.1. *Database analysis*

Version 5.11 of the Cambridge Structural Database (April 1996, 154 024 entries) was used in this study. Searches for covalent and non-covalently bonded substructures, and all geometry calculations, were carried out using the program *QUEST3D* (CSD: Cambridge Structural Database, 1994). Statistical analyses and data visualizations were performed with *VISA* (Cambridge Structural Database, 1995). All searches were restricted to those CSD entries that satisfied the secondary search criteria: (*a*) error-free coordinates after CSD evaluation procedures, (*b*) no reported structural disorder, (*c*) organic compound according to CSD chemical class definitions and (*d*) $R \leq 0.075$. The study of carbonyl···carbonyl interactions was restricted to ketonic $(C)_2$—C=O systems using the substructure search fragment of Fig. 1 and the non-covalent intermolecular 'group–group (*G*–*G*)' interaction search facility of the *QUEST3D* program. Atoms C1 and O2 were defined as *G*1, and C3 and O4 were defined as *G*2, and non-covalent intermolecular interactions were accepted if any atom of *G*2 was located within 3.6 Å of any atom of *G*1. The value of 3.6 Å was chosen as twice the van der Waals radius of carbon (Bondi, 1964) plus a tolerance value of 0.2 Å. For each fragment located, the program was instructed to output the two non-covalent C···O distances *B*1 and *B*2, the four angles *A*1–*A*4 and the torsion angle *T* = C1=O2···C3=O4, as depicted in Fig. 1; *T* is zero for an all-planar antiparallel arrangement of the two C=O groups.

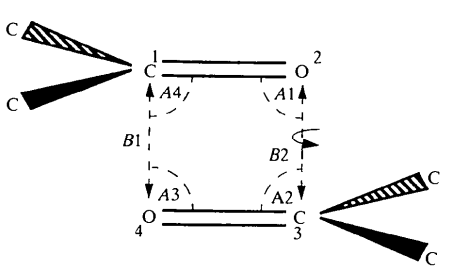

Fig. 1. Search fragment and geometrical parameters used in the analysis. Full details of the search process and the distance criteria used are given in the *Methodology*.

Owing to the atomic permutational symmetry of the search fragment (Fig. 1), it is impossible for the software to impose a unique atomic enumeration and so the output geometry table has the angle pairs *A*1, *A*3 and *A*2, *A*4 interchanged from hit to hit. Methods for circumventing this problem during the geometrical analysis of each individual interaction motif are indicated in the following sections. For the motifs (I, II, III) and with the atomic numbering of Fig. 1, *i.e.* with the top C=O bond numbered as C(1)=O(2) in each case, idealized angle sequences *A*1, *A*2, *A*3, *A*4 can be simply calculated; for a C=O distance of 1.2 Å and a C···O contact of 3.5 Å, they are

Motif (I)	75, 15, 180, 90°
Motif (II)	90, 90, 90, 90°
Motif (III)	90, 90, 55, 55°.

Other searches whose results are discussed below, *e.g.* for hydrogen bonds to ketonic O atoms from N—H or O—H donors, were carried out using *QUEST3D* and using the general methodologies described in detail elsewhere (see, for example, Allen, Baalham *et al.*, 1997) and with an O···H search constraint of 2.62 Å,

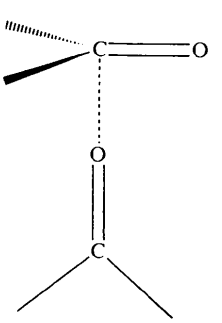

(I)

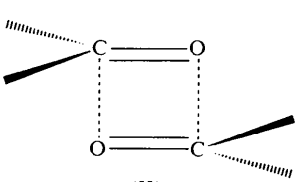

(II)

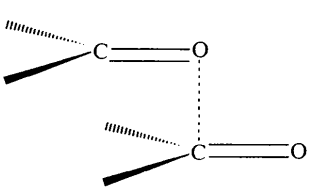

(III)

the sum of van der Waals radii for O (1.52 Å: Bondi, 1964) and H (1.1 Å, Rowland & Taylor, 1996).

2.2. *Molecular-orbital calculations*

The intermolecular perturbation theory (IMPT) of Hayes & Stone (1984), as implemented within the *CADPAC*6.0 program package (Amos, 1996), was used to quantify the carbonyl–carbonyl interaction energy. Applications of the IMPT method within *CADPAC*6.0 are fully described elsewhere (Lommerse *et al.*, 1996; Allen, Baalham *et al.*, 1997; Allen, Lommerse *et al.*, 1997) and only brief details are given here. Propanone was the model molecule used in this study and calculations were carried out using 6-31G** basis set functions. The model monomer was constructed and geometry optimized. Interacting propanone dimers were then constructed having various mutual orientations as described below. Intermolecular distances, other than those between the interacting C=O groups, were kept as long as possible to minimize possible C—H···O contributions to the total interaction energy. The IMPT method yields separate interaction energy terms which have a distinct physical significance and the sum of these terms yields a total interaction energy E_t, which is free of basis-set superposition errors (Stone, 1993). At first order the separate terms are E_{es}, the (attractive or repulsive) electrostatic energy, and E_{er}, the exchange–repulsion term. At second order the IMPT gives the polarization or induction energy E_{pol}, the charge-transfer energy E_{ct} and the dispersion energy E_{disp}.

All searches, data analyses and molecular-orbital calculations were carried out on SUN or Silicon Graphics workstations on the CCDC Unix network.

3. Analysis of crystal structure results

3.1. *Geometrical data from the complete CSD search*

A total of 9049 individual ketonic C=O groups were located in initial CSD searches, of which 2105 (24%) were involved in 1866 discrete non-covalent interactions within the search and distance criteria described above. The smaller of the two non-covalent C···O distances, *B*1 and *B*2, is displayed in the histogram of Fig. 2(*a*), while a representative angle histogram, for *A*2, is shown in Fig. 2(*b*) (other angle histograms are similar and are not shown here). The distance histogram shows that a significant proportion (538 or 29%) of the hits have both C···O distances ≥ 3.6 Å. These hits have been recorded due to either the C···C or the O···O distance falling within that rather broad distance criterion and such geometries are responsible for the occurrence of *A*2 values (Fig. 2*b*) that deviate considerably from the *ca.* 90° that would be associated with either the perpendicular (I) or antiparallel (II) interaction motifs. This point is demonstrated in the *A*2 histogram of Fig. 2(*d*), from which these data have been removed.

However, by far the greater proportion of hits (1328 or 71%) have one or both of their C···O distances < 3.6 Å and it is these hits that we now consider in some detail. In 346 cases (26%) the non-covalent C···O distance is less than 3.22 Å, the sum of van der Waals radii for C and O, and the overall median value is 3.35 Å. This is somewhat longer than the sum of van der Waals radii, but indicative, perhaps, of longer-range attractive interactions. The angle histograms of Figs. 2(*c*)–(*f*) now all show strong peaks in the region 80–100°, but with skewing towards higher (*A*1 and *A*3) and lower (*A*2 and *A*4) values. An explanation for the observed skewness of the angle distributions is afforded by analysis of the torsion angle *T* about the non-covalent C···O vectors.

Given that the rather tolerant 3.6 Å distance criterion of Fig. 1 is the only geometrical constraint used in the search, the shape of the $|T|$ histogram of Fig. 2(*g*) is, at first sight, quite remarkable: of the 1328 independent values of $|T|$, 650 (49%) lie within the narrow range from 0 to 20°. Examination of the search hits showed that 294 of the interacting pairs of keto groups were related to each other by a centre of symmetry, thus generating a torsion angle of exactly zero. However, there remain 356 instances of $|T| \leq 20°$ which are not dictated by local symmetry. More importantly, the skewness of the angle histograms for the 650 interaction patterns having $|T| < 20°$ is very significantly reduced (*cf.* Fig. 2*h* with Fig. 2*d* for angle *A*2), such that 553 of these fragments have all four angles *A*1–*A*4 within the range 60–120°. Mean values of the four angles taken over these 553 instances are 96.3 (4), 83.4 (4), 96.6 (4) and 83.6 (4)° for *A*1, *A*2, *A*3 and *A*4, respectively. These data correspond to an antiparallel interaction motif (II), which is sheared away from a perfect rectangle by *ca.* 6.5°, as illustrated in Fig. 3(*a*).

We then isolated examples of the perpendicular motif (I). To take account of the permutational symmetry problem identified in the *Methodology* section, the maximum value of *A*1 and *A*3 in any hit was constrained to lie in the range 150–180° and 116 fragments were located, 8.7% of the total. The mean values of angles *A*1–*A*4, now referred to a unique atomic enumeration (Fig. 3*b*), are 68.1 (11), 18.9 (10), 159.7 (7) and 97.2 (12)°, respectively. The enlargement of the *A*4 angle above 90° is, perhaps, unsurprising, in light of the work of Bürgi *et al.* (1974) on the direction of approach of oxygen nucleophiles to carbonyl centres.

Given that the angular geometry of (I) has one angle close to 180°, values of the torsion angle *T* are meaningless and are likely to be spread over the complete $|T|$ range. Thus, the sharp peak of more than 100 fragments close to 180° in the $|T|$ distribution of Fig. 2(*g*) must be attributed to the sheared parallel

motif (III). The ideal motif is characterized by angles $A1$–$A4$ of 90, 90, 55, 55° or 55, 55, 90, 90° (see *Methodology*), depending on the atomic enumeration selected by the CSD search procedure. To examine the experimental geometry of (III) we isolated those 179 fragments, 13.5% of the total, having $|T|$ in the range 160–180° and plotted angle histograms which all showed a bimodal distribution with peaks at *ca.* 50° and *ca.* 100°, the histogram for $A2$ (Fig. 4*a*) being typical. We then enforced a unique enumeration by

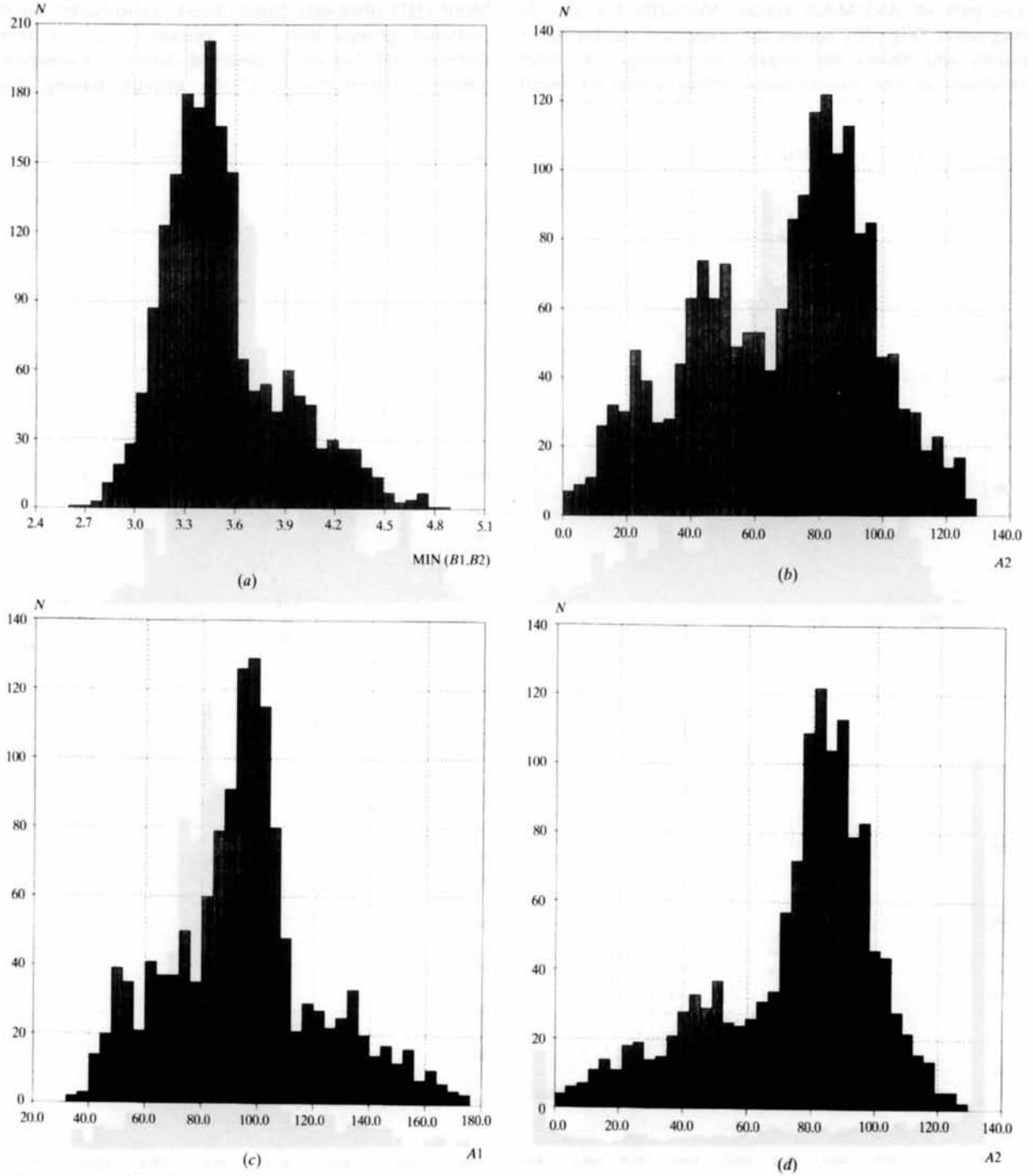

Fig. 2. Histograms of C═O···C═O interaction geometry: (*a*) Smaller of $B1$ and $B2$ (Å) for all data; (*b*) angle $A2$ (°) for all data; (*c*)–(*f*) $A1$, $A2$, $A3$ and $A4$ (°) for interactions having one or both of $B1$ and $B2 \leq 3.6$ Å; (*g*) $|T|$ (°) for this reduced dataset; (*h*) $A2$ (°) for the subset having $|T|$ in the range 0–20°.

taking the maximum and minimum values of the angle pairs $A1$, $A3$ and $A2$, $A4$. To display the data, we then averaged the two maximum values, essentially averaging all the values of $A1$–$A4$ under the 100° peak, and then averaged the two minimum values, essentially averaging all the $A1$–$A4$ values under the *ca.* 50° peak. The plot of AVEMAX *versus* AVEMIN for all 179 fragments (Fig. 4*b*) shows the expected clustering of points and shows the degree of slippage or shear exhibited in the experimental observations of motif (III). To obtain an average angular geometry (Fig. 3*c*) for this motif, those few values of $A1$–$A4$ that were $< 30°$ or $> 120°$ were excluded and the process described above was repeated. The mean values of AVEMAX and AVEMIN over the remaining 130 observations were 98.8 (7) and 48.6 (5)°, respectively. Motif (III) obviously brings the C substituents on the carbonyl groups into close proximity and it is no surprise that this small subset of data is (*a*) comprised almost exclusively of C=O groups having Csp^2

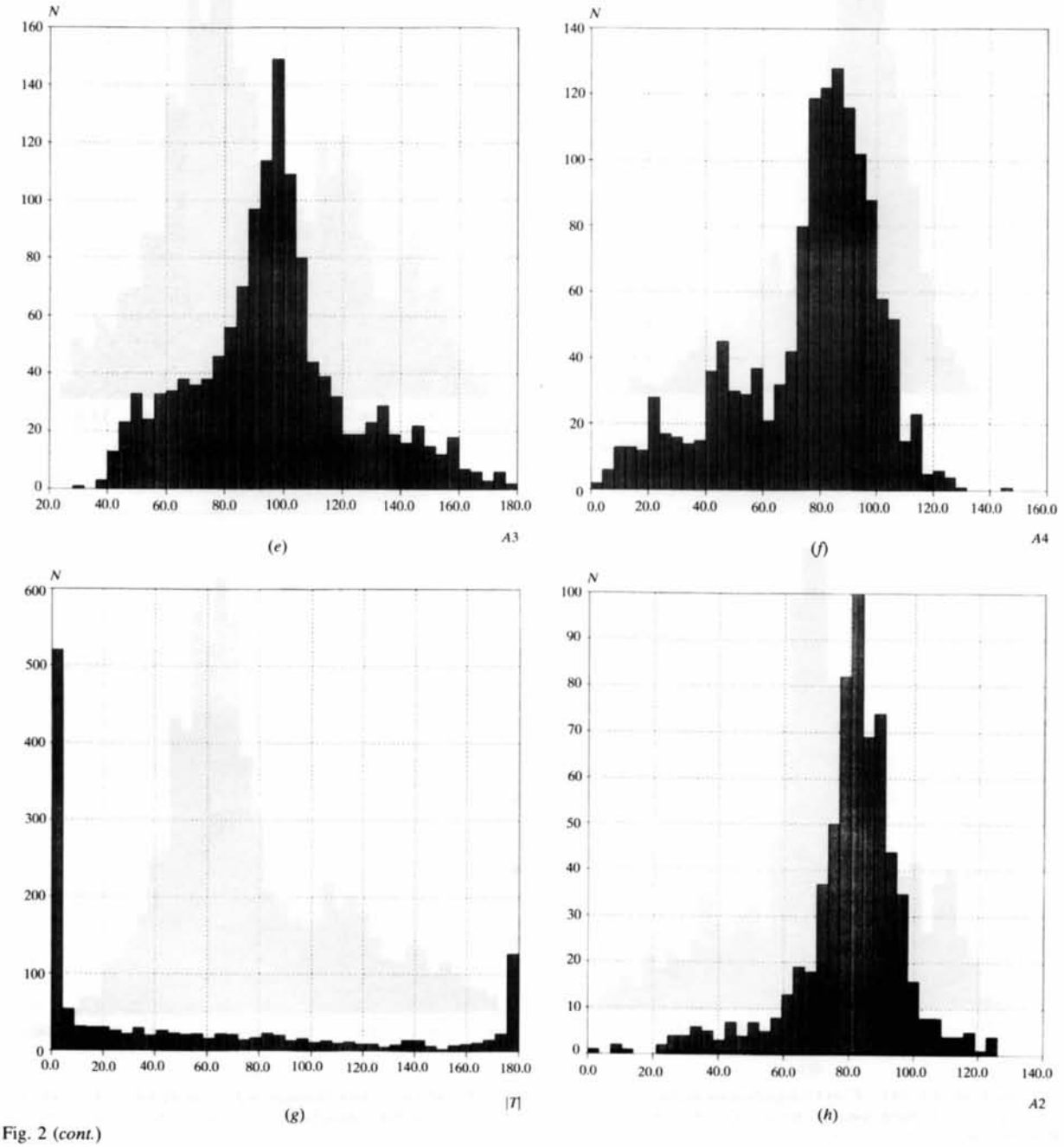

Fig. 2 (*cont.*)

(ethylenic or aromatic) substituents, usually with C═O *exo* to a planar delocalized ring system, which can then interact *via* π–π stacking, and (*b*) that the median C···O separation in motif (III) is 3.45 Å, rather longer than the 3.33 Å median observed for the antiparallel arrangement (II).

Analysis of the crystallographic data for C═O···C═O interactions shows that the experimental observations are dominated by the slightly sheared antiparallel motif [(II), Fig. 3*a*], the perpendicular motif [(I), Fig. 3*b*] and the sheared parallel motif [(III), Fig. 3*c*], which together account for 945 (71.1%) of the 1328 fragments having one or both of the C···O separations < 3.6 Å. The remaining 383 interactions all have $|T|$ in the range 20–160°, exhibit wide ranges of the angles *A*1–*A*4 and frequently have only one of the C···O distances within the 3.6 Å limit. They cannot be further categorized into clear motifs, but, rather, represent the full gamut of rotations and distortions of the 'singly C···O connected' motifs (I) and (III).

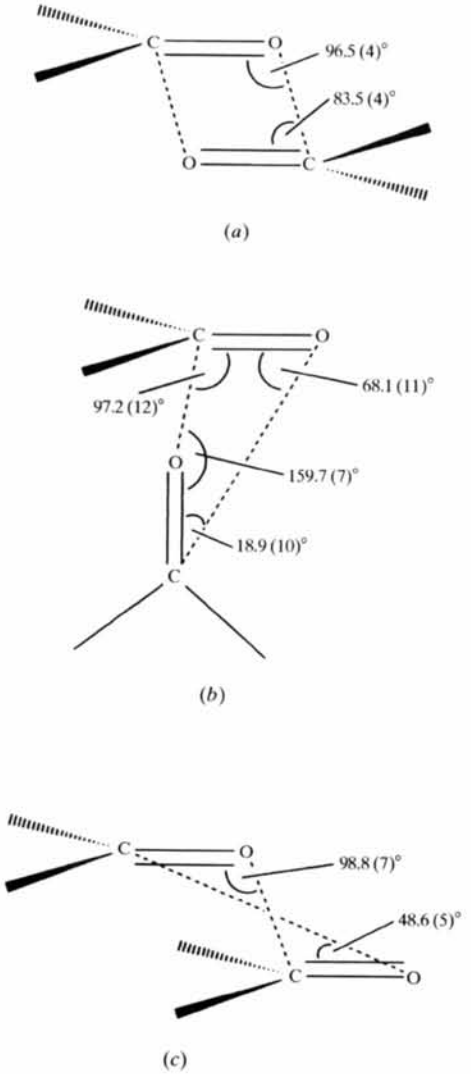

Fig. 3. Average geometries for the three most common motifs as determined from the database analysis (*a*) antiparallel motif, (*b*) perpendicular motif and (*c*) sheared parallel motif. Standard deviations *of the mean* are given with each.

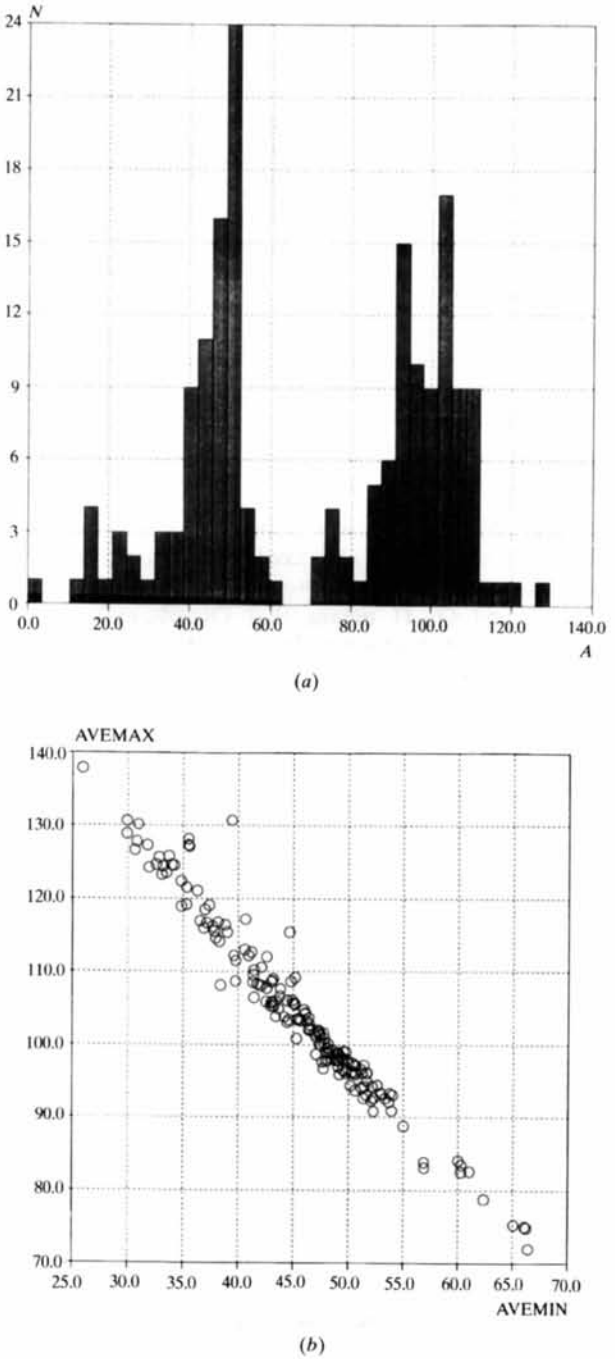

Fig. 4. The sheared parallel motif (III): (*a*) histogram of angle *A*2 (°); (*b*) scattergram of AVEMAX (°) *versus* AVEMIN (°), see text for definitions.

3.2. *Comparative frequency of C=O···C=O and C=O···H–N,O bond formation*

The analysis above shows that 15% of C=O groups form C=O···C=O interactions. By comparison, there are 3124 >C=O groups (having only C substituents) in the CSD that occur in crystal structures which also contain N–H or O–H donors. Of these, 1279 (41%) of the available C=O acceptors form hydrogen bonds within the van der Waals radii limit of 2.62 Å. The ratio of these two percentages (15/41) is 0.37. While comparative frequencies of non-covalent interactions from crystallographic data must be used with care in making estimates of relative interaction energies, it is reasonable to assume here that the average interaction energy of the various C=O···C=O [(I), (II), (III)] motifs is significantly less than the *ca.* -28 kJ mol^{-1} for >C=O···H–O or >C=O···H–N. In this case, however, it is particularly unwise to estimate even an approximate C=O···C=O interaction energy, since the principal motifs employ different numbers of C···O interactions in their formation.

3.3. *Geometrical data for structures containing only C, H and O (carbonyl)*

The CSD search was repeated with additional chemical criteria that restricted hits to structures that contained only C, H and O(carbonyl). The elimination of hydroxyl O–H means that O(carbonyl) is now prevented from forming hydrogen bonds stronger than C–H···O bonds. A total of 1227 C=O groups were located in this search, of which 383 took part in 345 C=O···C=O interactions within the distance criteria stated. After elimination of those hits that arose only from shorter O···O and C···C distances, a total of 309 C=O···C=O interactions remained in which one or both of the C···O interactions was less than 3.6 Å. Thus, a significantly higher proportion (25.2%) of C=O groups in this restricted subset form C=O···C=O interactions than in the general subset (14.7%) discussed above. While the lack of strong hydrogen-bonding options are the obvious reason for this increase, one might have expected it to be larger, especially in light of the energy calculations reported below. This subset is now being further analysed to systematize other intermolecular recognition mechanisms that may be present. The geometrical features of the carbonyl–carbonyl interactions in the subset are, nevertheless, very similar to those in the general dataset and are not discussed further.

4. Molecular-orbital calculations

4.1. *IMPT calculations*

Intermolecular perturbation theory calculations were carried out using two propanone molecules to form the model dimer. The geometry of an isolated molecule was first optimized using 6-31G** basis sets and the dimer was then constructed using the square antiparallel geometry depicted in Fig. 1. The IMPT method was used to study variations in the individual energy terms and, of course, the total interaction energy profile E_t as functions of (*a*) the separation distance between the C=O groups, *d*, which is equivalent to either of the C···O non-covalent distances in the rectangular arrangement depicted in Fig. 1, (*b*) the inter-vector angle O···C=O (*A*2 or *A*4 in Fig. 1) to study the effects of shearing of the motif and (*c*) as a function of the torsion angle *T* in the antiparallel arrangement. IMPT calculations were also performed for the perpendicular dimer motif (I) as a function of the (unique) C···O separation distance.

4.2. *Energy variation with d, the antiparallel carbonyl–carbonyl separation distance*

IMPT calculations were carried out for the nine fixed values of the carbonyl–carbonyl separation distance given by varying *d* from 2.82 to 3.62 Å in 0.1 Å increments. A tenth calculation was carried out at *d* = 3.07 Å, close to the computed energy minimum. Variations in the separate energy terms and E_t are shown in Fig. 5(*a*). The energy profile for E_t shows a shallow minimum from 2.92 to 3.32 Å having attractive energies below -20 kJ mol^{-1} and an absolute minimum of -22.3 kJ mol^{-1} at *d* = 3.02 Å. The graphs of the individual terms show that the minimum results from a balance between attractive electrostatic (E_{es}) and dispersion (E_{disp}) terms and the increasing exchange-repulsion term (E_{er}), with polarization (E_{pol}) and charge-transfer (E_{ct}) terms varying little from zero over the complete distance range sampled. The calculations confirm that the dipolar interaction is effective even at quite large distances, with an attractive E_t value as low as -16.5 kJ mol^{-1} being calculated at *d* = 3.62 Å. Obviously two small propanone molecules can achieve closer carbonyl···carbonyl contact distances than many of the molecules retrieved in the CSD searches, where steric factors in larger systems will tend to mitigate against the formation of close contacts. However, even at longer distances, the strength of the dipolar interaction is comparable to that of a medium-strength hydrogen bond and about half that of a strong hydrogen bond, *e.g.* C=O···H–O (Jeffrey & Saenger, 1991).

4.3. *Energy variation with shearing of the antiparallel motif*

IMPT calculations were carried out at nine fixed points as the angle *A*2 (Fig. 1) was varied from 70 to 110° in 5° steps. These calculations were carried out at three carbonyl–carbonyl separation values, *d* = 3.02, 3.12 and 3.22 Å, and the results are illustrated graphi-

cally in Figs. 5(*b*)–(*d*). The E_t profile at all three d values again reflects a balance between attractive E_{es} and E_{disp} components and the repulsive E_{er} component. At d = 3.02 Å (Fig. 5*b*) E_t remains below −20 kJ mol^{-1} over the range 82–100°, with the absolute energy minimum computed at 90°, corresponding to a perfectly rectangular planar motif. However, as d is increased through 3.12 to 3.22 Å, the position of the minimum moves to angles slightly greater than 90°: interpolation of the calculated E_t values indicates $A1 \simeq 93°$ at d = 3.12 Å and $A1 \simeq 96°$ at d = 3.22 Å, an indication that the slightly sheared motifs observed in crystal structures (Fig. 3*a*) may be energetically preferred at the longer d values which are observed in the CSD data.

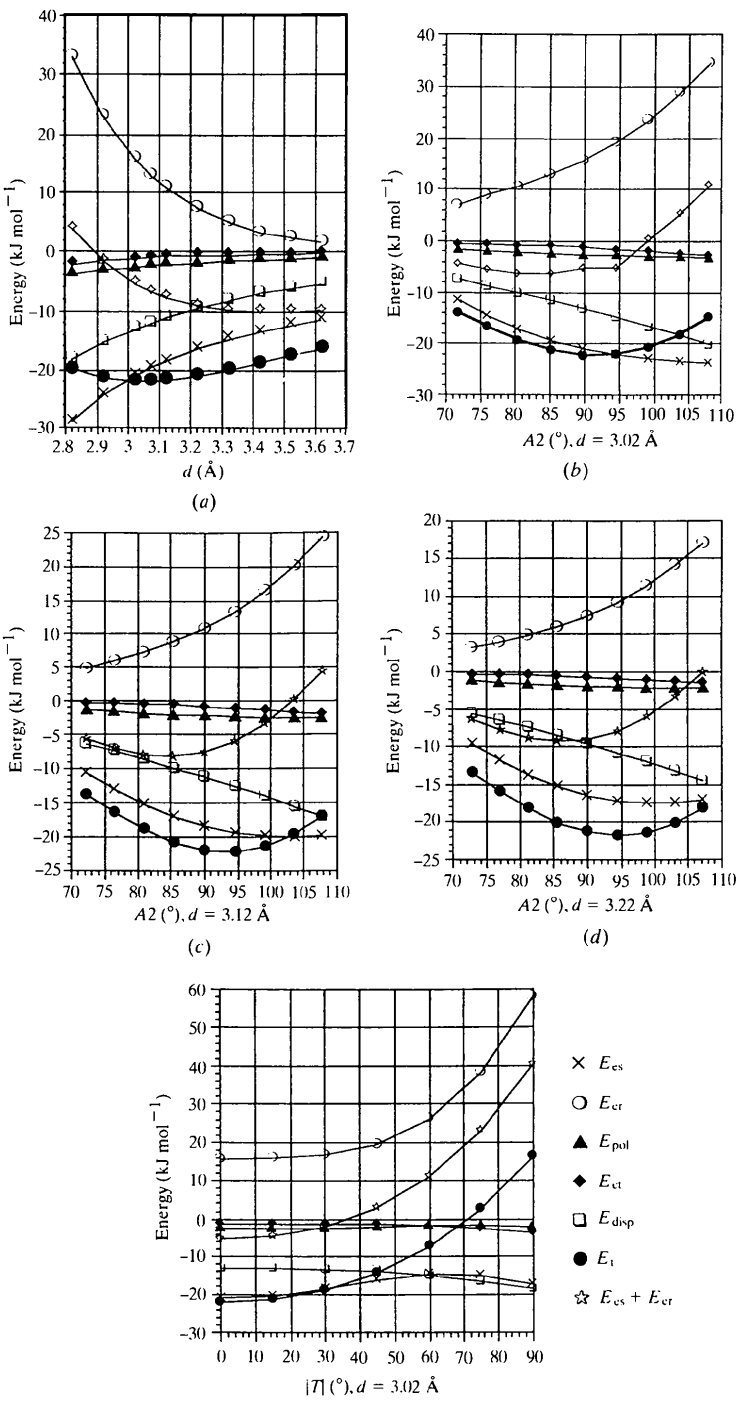

Fig. 5. IMPT energies for the anti-parallel motif (II): (*a*) energy variation with the C=O···C=O separation distance d, (*b*), (*c*), (*d*) energy variation with angle $A2$ at three different d values and (*e*) energy variation with the absolute value of the torsion angle $|T|$. Distances are in Å, angles in °.

4.4. *Energy variation with the C=O···C=O torsion angle T in the antiparallel motif*

The torsion angle T was varied from 0 to 90° in 10° steps and IMPT calculations were run at each step with a fixed d value of 3.02 Å. The results are presented graphically in Fig. 5(*e*). Here, there is little variation in any of the individual energy terms, except E_{er} as one C=O group is rotated with respect to the other and the E_t profile follows that of E_{er} almost exactly. There is a very small increase in E_t over the range T = 0–30°, from −22.3 to −19.1 kJ mol^{-1}, however, E_t then increases quite rapidly and becomes repulsive at T > 70°, the point at which the methyl groups of one propanone molecule begin to interact unfavourably with those of the other. There is no doubt that T = 0° is the preferred arrangement and for obvious reasons.

4.5. *Energy calculations for the perpendicular motif (I)*

IMPT calculations were performed for the perpendicular interaction motif (I) for three values of the unique C···O separation, d = 2.92, 3.02 and 3.07 Å, covering the area of minimum energy observed in Fig. 5(*a*). The E_t profile, illustrated graphically in Fig. 6, is again controlled by the balance between attractive E_{es} and E_{disp} components and the increasing exchange–repulsion term E_{er} as d shortens. E_t values of −7.4, −7.6 and −7.5 kJ mol^{-1} were obtained at the three chosen d values, an identical trend to that observed in Fig. 5(*a*), and the c.p.u.-intensive calculations were not extended to higher values of d, nor did we study variations in the interaction energy with changes in the angle of approach, O···C=O. Thus, the attractive C=O···C=O interaction energy for motif (I) is approximately one-third of that obtained for the antiparallel arrangement (II). Since the sheared parallel motif (III) also exhibits only one non-covalent C···O interation, it is reasonable to assume that the interaction energy here is similar to that in (I), although further interactions between the substituents on the >C=O bonds, referred to above, may enhance the overall interaction energy in specific structures and may be an underlying cause for the slightly greater population of motif (III) compared with that of motif (I). Another possible reason for this population imbalance is that the O atoms of the two >C=O groups in (III) are both exposed, so that both can take part in additional hydrogen bonding or other interactions. This is not true of motif (I).

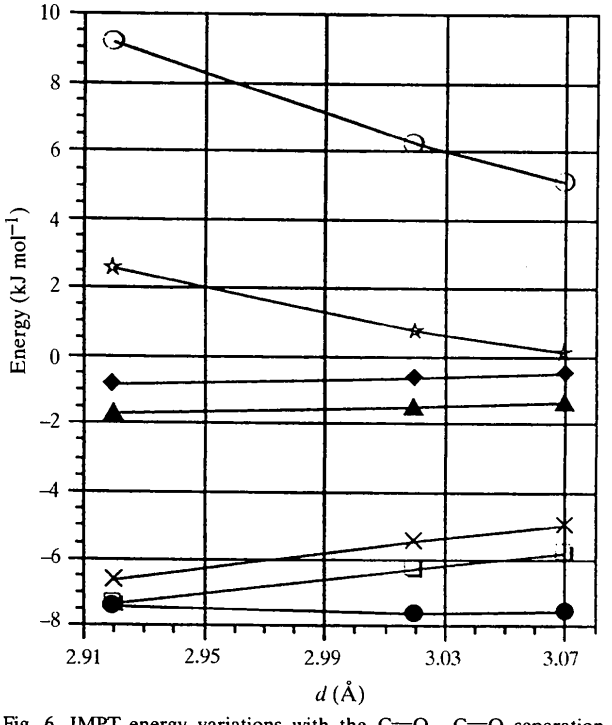

Fig. 6. IMPT energy variations with the C=O···C=O separation distance d (Å) in the perpendicular motif (II).

5. Conclusions

The combination of systematic database analysis and high-level *ab initio* molecular-orbital calculations is again shown to be highly effective in the study of non-covalent interactions. The results obtained here quantify the importance of dipolar interactions between carbonyl groups in stabilizing the packing modes of small organic molecules and confirm that the contribution of these interactions to supramolecular recognition processes is comparable to that of medium-strength hydrogen bonds. Our small molecule results are in complete agreement with the observations and calculations of Maccallum *et al.* (1995*a*,*b*) and add credence to their conclusion that C=O···C=O interactions are of significance in stabilizing protein secondary structure motifs. It is to be hoped that similar studies of dipolar, as distinct from hydrogen-bonded, interactions will reveal other strong non-covalent systems that also play similar crucial roles in stabilizing both the extended crystal structures of small molecules and the secondary structure motifs commonly observed in proteins.

We thank Dr Anthony Stone and Dr Roger Amos (University of Cambridge) for access to *CADPAC*6.0 and for advice on the IMPT method. We also thank the European Communities for financial support to JPML under the Training and Mobility of Researchers Programme, Contract No. ERB-CHR-XT-94-0469 (Molecular Recognition Network).

References

Allen, F. H., Baalham, C. A., Lommerse, J. P. M., Raithby, P. R. & Sparr, E. (1997). *Acta Cryst.* B**53**, 1017–1024.

Allen, F. H., Davies, J. E., Galloy, J. J., Johnson, O., Kennard, O., Macrae, C. F., Mitchell, E. M., Mitchell, G. F., Smith,

J. M. & Watson, D. G. (1991). *J. Chem. Inf. Comput. Sci.* **31**, 187–204.
Allen, F. H., Lommerse, J. P. M., Hoy, V. J., Howard, J. A. K. & Desiraju, G. R. (1997). *Acta Cryst.* B**53**, 1006–1016.
Amos, R. D. (1996). *CADPAC*6.0. *The Cambridge Analytical Derivatives Package. A Suite of Quantum Chemistry Programs.* Issue 6. Department of Chemistry, University of Cambridge, Lensfield Road, Cambridge, England.
Bernstein, J., Cohen, M. D. & Leiserowitz, L. (1974). *The Chemistry of Quinonoid Compounds*, edited by S. Patai, pp. 83–105. Wiley: London.
Bolton, W. (1963). *Acta Cryst.* **16**, 166–173.
Bolton, W. (1964). *Acta Cryst.* **17**, 147–152.
Bolton, W. (1965). *Acta Cryst.* **18**, 5–10.
Bondi, A. (1964). *J. Phys. Chem.* **68**, 441–451.
Bürgi, H.-B., Dunitz, J. D. & Shefter, E. (1974). *Acta Cryst.* B**30**, 1517–1523.
Cambridge Structural Database (1994). *User's Manual. Getting Started with the CSD System.* Cambridge Crystallographic Data Centre, 12 Union Road, Cambridge, England.
Cambridge Structural Database (1995). *VISTA*2.0 *User's Manual.* Cambridge Crystallographic Data Centre, 12 Union Road, Cambridge, England.
Gavezzotti, A. (1990). *J. Phys. Chem.* **94**, 4319–4325.
Hayes, I. C. & Stone, A. J. (1984). *J. Mol. Phys.* **53**, 83–105.
Jeffrey, G. A. & Saenger, W. (1991). *Hydrogen Bonding in Biological Systems.* Berlin: Springer-Verlag.
Lommerse, J. P. M., Stone, A. J., Taylor, R. & Allen, F. H. (1996). *J. Am. Chem. Soc.* **118**, 3108–3116.
Maccallum, P. H., Poet, R. & Milner-White, E. J. (1995*a*). *J. Mol. Biol.* **248**, 361–373.
Maccallum, P. H., Poet, R. & Milner-White, E. J. (1995*b*). *J. Mol. Biol.* **248**, 374–384.
Rowland, R. S. & Taylor, R. (1996). *J. Phys. Chem.* **100**, 7384–7391.
Stone, A. J. (1993). *Chem. Phys. Lett.* **211**, 401–409.
Taylor, R., Mullaley, A. & Mullier, G. W. (1990). *Pestic. Sci.* **29**, 197–213.